Publications of the Astronomical Society of the Pacific, 134:061001 (9pp), 2022 June https://doi.org/10.1088/1538-3873/ac6e4c

On the Determination of the Evolutionary Status of Supernova Remnants from Radio Observation Data

Dejan Urošević
Department of Astronomy, Faculty of Mathematics, University of Belgrade, Studentski trg 16, 11000 Belgrade, Serbia; dejanu@math.rs
Received 2021 May 31; accepted 2022 May 9; published 2022 June 21

Abstract

This paper aims to give a brief review of a new concept for the preliminary determination of the evolutionary status of supernova remnants (SNRs). Data obtained by radio observations in continuum are used. There are three different methods underlying the new concept: The first one is based on the location of the observationally obtained radio surface brightness and the corresponding diameter of an SNR in theoretically derived Σ–D tracks, the second one is based on the forms of radio spectra, and the third one is based on the magnetic field strengths that are estimated through the equipartition (eqp) calculation. Using a combination of these methods, developed over the last two decades by the Belgrade SNR Research Group, we can estimate the evolutionary status of SNRs. This concept helps radio observers to determine preliminarily the stage of the evolution of an SNR observed in the radio domain. Additionally, this concept was applied to several SNRs, observed by the Australia Telescope Compact Array, and the corresponding results are reviewed here. Moreover, some of the results are revised in this review to reflect the recently published updated Σ–D and eqp analyses.

Unified Astronomy Thesaurus concepts: Radio continuum emission (1340); Supernova remnants (1667)

Online material: color figure

1. Introduction

Radio continuum observations of supernova remnants (SNRs) help us obtain directly their flux densities and angular extensions. From these two quantities, we can easily calculate the so-called surface brightness Σ, which is a distance-independent quantity. The surface brightness of an SNR changes over time. On the other hand, with time propagation, the volume of an SNR (defined by an approximately spherical shock wave that separates the object and surrounding interstellar medium) increases. If we assume an SNR is of a spherical form, we can define its diameter D. As a result, the evolution of an SNR can be described by changes in the surface brightness with the increase of its diameter i.e., by the so-called Σ–D relation. This method based on the radio surface brightness evolution of an SNR with the increase of its diameter is the first ingredient of the concept, introduced in this review, for determining the evolutionary status of an SNR. The second one relates to the different forms of SNR radio continuum spectra. The radio continuum spectra of SNRs are derived from observations in different frequency bands—they are defined by the values of the flux densities at different frequencies. A spectrum is better if we can provide more observations at different frequencies. The forms of SNR radio spectra are different in different stages of evolution of an SNR. Due to this, we can estimate the evolutionary status of an SNR from a careful analysis of its spectrum. Finally, the third method is connected to the equipartition (eqp) calculation of magnetic field strengths in SNRs—namely, younger SNRs have conditions for higher magnetic fields, while older SNRs have lower magnetic fields. Each of these three methods is based on the diffusive shock acceleration (DSA) theory. This type of particle acceleration is responsible for the production of cosmic rays (CRs) at the SNRs' strong shock waves. All of these three methods are presented in detail in the next three sections of this review, respectively. In Section 5 the concept of the combined use of these three methods for determining the evolutionary status of SNRs is given. Examples from published papers (the first one in 2012) in which this new concept is applied are presented in Section 6. Pavlović et al. (2018) and Urošević et al. (2018) reanalyzed the Σ–D and eqp methods and due to these new results, the estimated evolutionary statuses from Section 6 (eight SNRs; papers published from 2012 to 2018) are revised in Section 7. Section 8 summarizes the previously presented information. The short version of this study was presented in Urošević (2020), where only the fundamental ideas of the new concept were given.

2. Σ–D Tracks

The Σ–D relation for SNRs was defined by Shklovskii (1960a, 1960b) in two directions: as a method to describe the SNR radio surface brightness evolution and as a method to determine the distances to SNRs. This relation was studied for

almost 60 yr, with activity, more or less, in individual decades. The first four decades of development of Σ–D studies are reviewed in Urošević (2000, 2002, 2005). In the last two decades, Urošević et al. (2003a, 2003b), Berezhko & Völk (2004, hereafter BV04), Urošević & Pannuti (2005), Bandiera & Petruk (2010), Pavlović et al. (2013), and Pavlović et al. (2018) developed the theoretical concepts in Σ–D studies. The authors who worked on the development of the empirical relations in the last two decades include Guseinov et al. (2003), Urošević (2003), Arbutina et al. (2004), Arbutina & Urošević (2005), Urošević et al. (2005, 2010), Bandiera & Petruk (2010), Pavlović et al. (2013, 2014), Vukotić et al. (2014), Kostić et al. (2016), Bozzetto et al. (2017), and Vukotić et al. (2019).

As mentioned in the introduction, the radio surface brightness is a quantity independent of the distance to the object. Here we encounter the first problem in this method because to calculate the diameter, we also need the distance to the object. For extragalactic samples of SNRs, this problem does not exist—all SNRs in one galaxy are at the same distance equal to the distance between us and that galaxy. This problem, however, does exist for the Galactic SNR sample. We do not have precise methods for estimating SNR distances in our Galaxy. Due to this, the diameter of an SNR can be estimated only with significant uncertainty. There are several independent methods (not based on the Σ–D relation) for determining distances to Galactic SNRs. We can use the SNRs with independently determined distances for the creation of a calibration sample. For the calibration sample, we can set the Σ–D relation and use this relation to estimate the distances to SNRs for which we do not have independently determined distances. Around 100 SNRs in the Galactic sample have independently determined distances, but for approximately 200 of them, we have to use the Σ–D relation in order to determine their distances (for details, see Vukotić et al. 2019).

In this review, we examine how the radio surface brightness of an expanding SNR evolves, i.e., the corresponding Σ–D dependence. The main idea behind the method to determine the evolutionary status of an SNR by using Σ–D tracks is based on theoretically derived changes in the radio surface brightness of an expanding SNR (forming of evolutionary paths). For initial conditions, we can set the values for the explosion energies of supernovae and values for the densities of surrounding media in which SNRs expand. For different combinations of energies and densities, we can obtain different evolutionary paths. For extragalactic SNRs, the radio surface brightness and diameter are obtained directly from observations—diameters can be easily calculated if we know the distance to the host galaxy. If we analyze a Galactic SNR, the distance should be estimated first (by using some independent method or the Σ–D relation) and then we should calculate the diameter. An observed SNR with the determined values for Σ and D can be shown in the Σ–D plane, and after examining which evolutionary path this SNR is located at, we can estimate its evolutionary status, environmental density, and SN explosion energy.

BV04, in their theory of synchrotron emission from SNRs, presented for the first time the evolutionary paths in the Σ–D plane. This analysis is based on the time-dependent nonlinear kinetic theory for particle acceleration in SNRs. They used numerical calculations performed for the expected range of ambient densities and SN explosion energies. The magnetic field in SNRs is assumed to be significantly amplified by nonlinear DSA effects.

In the next and last analyses of the radio evolution of SNRs based on the nonlinear kinetic theory of CR acceleration coupled with three-dimensional hydrodynamic simulations, Pavlović et al. (2018, hereafter P18) took a new approach to the creation of evolutionary Σ–D tracks. They performed simulations for a wide range of the relevant physical parameters, such as ambient density, SN explosion energy, acceleration efficiency, and magnetic field amplification (MFA) efficiency. A detailed description of the supercomputer simulations applied in the creation of Σ–D tracks is given in P18.

The Σ–D diagrams presented in the previous two papers can be used to determine the evolutionary status of an observed SNR. The evolutionary paths in P18 are obtained by using an advanced approach, and due to this, they are better for further use.

3. Forms of Radio Spectra

The second method that can be used to determine the evolutionary status of SNRs is based on the analysis of the forms of SNR continuum radio spectra. The details on the SNR radio spectral forms can be found in Urošević (2014). Here, only a brief review is presented. Young SNRs have steeper spectral indices with $\alpha > 0.5$ ($S_\nu \propto \nu^{-\alpha}$, where S_ν is the flux density at the observed frequency ν). These steeper spectral indices are the result of nonlinear particle acceleration effects incorporating strong MFA (for details, see Urošević 2014; Pavlović 2017; Bell et al. 2019). Also, the radio spectra of young SNRs can be curved (concave up)—again, it is the effect of the nonlinear DSA, i.e., the modification of the shock front (for details, see Urošević 2014 and Onić & Urošević 2015). Also, the steep linear or curved spectra frequently appear for the evolved SNRs. The test particle DSA predicts linear spectra for older SNRs with spectral indices around 0.5, and they should be steeper with further SNR evolution. Mostly, the evolved SNRs have spectral indices in the interval $0.5 < \alpha < 0.6$. Additionally, curved, concave-up spectra can be expected for evolved SNRs where a significant amount of thermal bremsstrahlung radiation can be added to the synchrotron radiation. The evolved SNRs in some cases show concave-down spectra. This kind of spectrum can be explained using DSA theory with the effect of synchrotron losses within

the finite emission region. Also, for details on the spectra of evolved SNRs, see Urošević (2014).

Forms of radio spectra can be used to determine the evolutionary status of an SNR, i.e., determining whether it is young or evolved. For easier reference, see Table 1 in Urošević (2014).

4. The Magnetic Field Strengths

Relying on data obtained by radio observations, with the additionally provided distance to an SNR, and using the eqp calculation, we can estimate the magnetic field strengths. This method was suggested by Pacholczyk (1970). The modification of the original method was given by Beck & Krause (2005). The development of the eqp method applied to SNRs was started by Vukotić et al. (2007) and continued by Arbutina et al. (2012, 2013) and Urošević et al. (2018). The eqp method is based on the calculation of the value of the magnetic field strength for which the total energy density in the system is minimal (part of the total energy density is necessary for synchrotron emission). This total energy density has two ingredients: the energy density of CRs and the energy density of magnetic fields. The minimal energy requirement is equivalent to the eqp assumption—it means that energy densities of CRs and magnetic fields are approximately equal (eqp). Additionally, these two energy densities can be in any constant partition (Arbutina et al. 2012; Urošević et al. 2018) and used to determine magnetic field strengths. In a recent paper from this series, Urošević et al. (2018) showed that the eqp (or the constant partition) between ultrarelativistic electrons and magnetic fields represents the best starting assumption for estimating the magnetic field strengths in SNRs. This is shown by using 3D hydrodynamic supercomputer simulations, coupled with a nonlinear DSA model. However, the eqp method can be used only for the estimation of magnetic field strengths with an order-of-magnitude precision. For our purposes—determining the evolutionary status of an observed SNR—the order-of-magnitude determination is precise enough. In young SNRs, where shocks are very strong, nonlinear DSA effects can provide conditions for MFA. The magnetic field amplification in modified shocks can be 100 times higher than that by the compression-obtained fields in nonmodified shocks. The magnetic fields made only by shock compression can be at most four times higher than interstellar (IS) magnetic fields (the average value of the IS magnetic field is around 5 μG). Due to this, the order of magnitude of a few tens of microgauss should correspond to the magnetic fields of evolved SNRs. For young SNRs, the characteristic values are a few to several hundred microgauss. All of these estimates depend on the density of the environment. Discussion on the dependence between the density of the environment and magnetic field strength is presented in Sections 6 and 7.

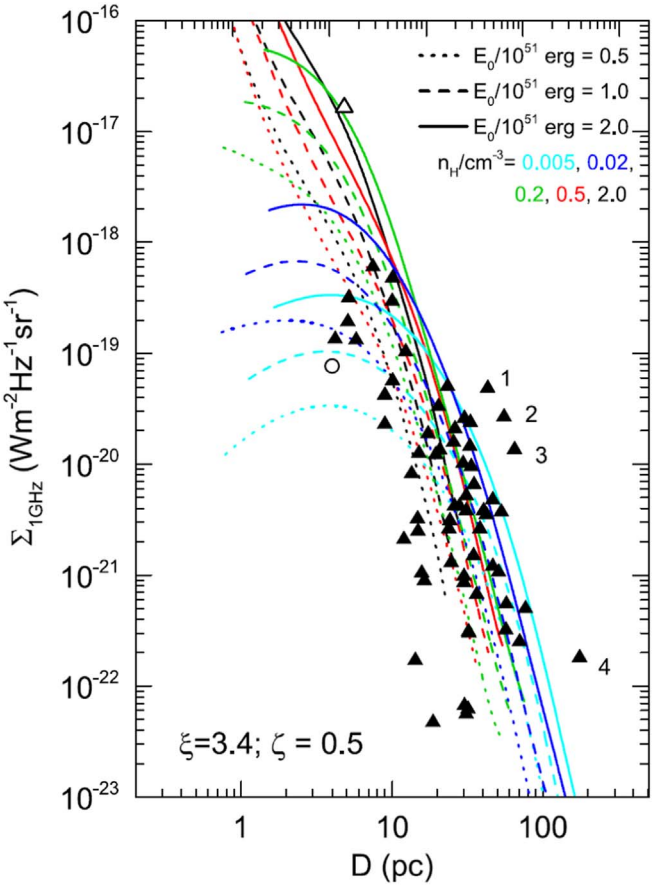

Figure 1. Σ–D diagram for SNRs at 1 GHz from P18.

The calculation of magnetic field strengths from the eqp model is a rather straightforward process. An observer should provide data obtained from observations: the radio flux density at a radio frequency for an SNR, spectral index, distance, and volume filling factor (part of the volume of an SNR from which we see synchrotron emission—the volume of the shell). User should enter the data on the web page: http://poincare.matf.bg.ac.rs/~arbo/eqp/, and the calculator[1] will return the eqp magnetic field strength and the minimum total energy. The formulae implemented in this calculator and the corresponding detailed explanations can be seen in three papers: Arbutina et al. (2012, 2013) and Urošević et al. (2018).

5. Determination of Evolutionary Status—A New Concept

To determine the evolutionary status of an observed SNR in the radio spectrum, we can start with a Σ–D analysis. The theoretically derived evolutionary paths from P18 are shown in Figure 1. In this figure, different line colors correspond to

[1] Use $\kappa = 0$ for electron eqp, or $\kappa \neq 0$ for CR eqp.

Table 1
Revised Table 1 from Urošević (2014)

Theoretical Predictions					
	Linear Radio Spectra			Curved Radio Spectra	
	$\alpha = 0.5$	steep ($\alpha > 0.5$)	flat ($\alpha < 0.5$)	concave-up	concave-down
Young SNRs	test particle DSA	ampl. mag. field + quasi-perp. shocks	DSA + Fermi 2	nonlinear DSA	obs. effects + DSA effects
Evolved SNRs	DSA	test particle DSA	DSA + Fermi 2	synch. + brem. or spin. dust	obs. effects + DSA effects
From Observations					
	Linear Radio Spectra			Curved Radio Spectra	
	$\alpha = 0.5$	steep ($\alpha > 0.5$)	flat ($\alpha < 0.5$)	concave-up	concave-down
Young SNRs	/	e.g., Cas A, G1.9+0.3	/	e.g., Cas A, Tycho, Kepler, SN1006	/
Evolved SNRs	e.g., Monoceros and Lupus loops	e.g., HB3, HB9	e.g., W28, Kes67, 3C434.1	e.g., IC443, 3C391, 3C396	e.g., S147, HB21, J0455-6838

Note. The theoretically predicted radio spectra and some examples for observational spectra of shell, composite, and mixed-morphology SNRs.

different ambient densities, $n_H/\mathrm{cm}^3 = 0.005$ (cyan), 0.02 (blue), 0.2 (green), 0.5 (red), and 2.0 (black). Dotted, dashed, and solid lines correspond to different explosion energies, namely, $E_0/10^{51}$ erg = 0.5 (dotted), 1.0 (dashed), and 2.0 (solid). Observational data marked with triangles represent the 65 Galactic SNRs with known distances taken from Pavlović et al. (2014). They represent the evolutionary tracks for injection parameter $\xi = 3.4$ and nonlinear magnetic field damping parameter $\zeta = 0.5$. For more details, see P18. SNR Cassiopeia A (Cas A) is marked with an open triangle, while the youngest Galactic SNR, G1.9+0.3 (see Pavlović 2017 for detailed modeling) is marked by an open circle. Numbers represent the following SNRs: (1) CTB 37A, (2) Kes 97, (3) CTB 37B, and (4) G65.1+0.6.

A line in Figure 1 represents an evolutionary path for one combination of the SN explosion energy and the ambient density. The ascending part of the evolutionary track represents the evolution of a very young SNR in the early free expansion phase. When the line starts to decline, this corresponds to late free expansion, and after that, the SNR enters the early Sedov phase of evolution. When the steepness of the evolutionary path becomes highest and has a constant slope, this part corresponds to the Sedov phase of evolution. The lines finish at the end of the late Sedov phase. The simulations presented by these Σ–D tracks do not cover the radiative phases of evolution.

If radio observers detect a new SNR in radio and calculate its corresponding surface brightness and diameter, they can use Figure 1 to locate their SNR somewhere in the Σ–D plane. Depending on which part of the curved evolutionary path the targeted SNR is located in, observers can determine the phase of evolution for their SNR. They can also estimate the relevant ambient density and SN explosion energy.

On the other hand, the evolutionary paths in Figure 1 are very close and intercept each other. Due to this, we are not sure if we have a unique Σ–D track for an SNR. We therefore move to the next method and check the form of the spectrum of a newly observed SNR. As mentioned in Section 3, we should check the spectral index value, or whether or not the spectrum is curved, and by using Table 1 and the analysis in Urošević (2014) we can obtain more information on the evolutionary status of an SNR—whether the SNR is young or evolved. This is one more method that can be combined with the Σ–D track method.

Additionally, concave-up spectra can represent young SNRs, but they can also represent evolved ones (see Section 3 and Table 1). Also, spectral index slopes steeper than 0.5 are a consequence of the strong nonlinear effects at the start of the SNR evolution, but for SNRs that are evolved, steeper spectral slopes may be due to the low efficiency of particle acceleration. If a mix of the Σ–D and spectral form methods does not lead to a single conclusion, we should resort to the eqp calculation in order to establish magnetic field strengths. As explained in Section 4, observers should prepare data on which they can very easily calculate the values of the SNR magnetic fields. The higher the magnetic field, the younger the newly observed SNR. Overall, we can make a preliminary determination of the evolutionary status of an SNR with optimal reliability if we

combine the three methods. This combination of methods represents the new concept introduced in this review.

To check how this concept works, we will look at the youngest two Galactic SNRs: Cas A (approximately 330 yr old) and G1.9+0.3 (120 yr old). Both SNRs were studied many times and we know in which phases of evolution they are.

In Figure 1, Cas A is shown by an open triangle, and G1.9 +0.3 is shown by a circle. We can estimate the evolutionary status of Cas A by using Figure 1: young SNR, expansion in an environment between average and higher density, SN explosion energy is higher than average. The spectral index is very steep, 0.77, and the spectrum appears to be slightly concave up —this suggests that Cas A is a very young SNR in which the characteristic spectral forms are due to nonlinear effects (see Onić & Urošević 2015). The electron eqp magnetic field strength is 760 μG (Urošević et al. 2018). According to the concept presented in this review, Cas A is a young SNR in the late free expansion phase (for higher than average environmental density, SNRs do not show the ascending part of surface brightness evolution (P18)). This conclusion is in very good agreement with earlier confirmed facts on Cas A: It is an extremely bright Galactic SNR in the free expansion phase, a so-called oxygen-rich SNR that evolves in a high-density medium ($\sim$3 cm^{-3}; see Arbutina & Urošević 2005 and references therein), with an average magnetic field strength of $>$500 μG (Vink & Laming 2003). The evolutionary paths from Figure 1 give a slightly lower density in which Cas A expands and therefore a slightly older evolutionary status.

For the youngest Galactic SNR, the position of G1.9+0.3 in Figure 1 suggests the free expansion phase of evolution in a very rare environmental density with average SN explosion energy. The spectral index is steep, $\sim$0.8 (Luken et al. 2020), and the electron eqp suggests a magnetic field strength of 75 μG. This estimate is in good agreement with earlier confirmed facts for G1.9+0.3. We estimate here a four times lower density in which this SNR expands and, due to this, also an older evolutionary status. Pavlović (2017) presented that G1.9 +0.3 is in the rising part of its evolution. In the present period, approximately 120 yr after explosion, it seems that we are witnessing approximately the fastest radio emission increase that will ever be. The rising part of the evolution will continue in the next 500 yr. From Figure 1, we can conclude that G1.9 +0.3 is around maximal surface brightness, and therefore, we can estimate that it is an evolutionary older SNR—not in the rising part of the free expansion evolution, but in the period of maximal brightness.

Both SNRs are very young and therefore the eqp (or constant partition) is not a valid assumption for the calculation of the magnetic field value in the present moment of evolution, especially for G1.9+0.3 (see Urošević et al. 2018), but after 10 kyr in the future, it will be. Directly from the simulations, Urošević et al. (2018) obtained a magnetic field strength of 300 μG. An interesting fact to note here, for both eqp values, is that they are approximately on the order of magnitude to the correct values obtained earlier, especially for Cas A.

Additionally, Cas A and G1.9+0.3 are not standard SNRs in order of their place on the radio surface brightness to diameter diagram. Cas A is an extremely bright Galactic SNR, while G1.9+0.3 is a low-brightness object given its diameter (see Figure 1). Due to this, we choose extreme objects and generally capture reliable evolutionary phases for them. We miss the subphase for G1.9+0.3.

The concept presented here is based on supercomputer simulations that do not cover the radiative phases of SNR evolution. As stated in Raymond et al. (2020), the simple adiabatic compression of the ambient CR population, along with compression of the gas and magnetic field downstream of a radiative shock, could provide significant radio synchrotron emission. Due to this, in the radiative shocks, DSA and turbulent acceleration of CRs, such as the turbulent amplification of the magnetic field, should not be important for the production of radio emission. Also, Tutone et al. (2021) suggested that reacceleration of preexisting ambient CRs provides conditions for efficient synchrotron radiation from these low-velocity shocks ($v_s < 150$ km s^{-1}). In accordance with the predicted higher compression ratios on SNR shocks in the radiative phases of evolution (depending on the square of the shock Mach number), the radio spectral indices should be lower than 0.5 (for details, see Onić 2013; Urošević 2014). Additionally, old SNRs embedded in higher-density medium can produce thermal bremsstrahlung radiation, which can make flatter or concave-up spectra (Urošević et al. 2007; Onić et al. 2012). Moreover, the high compression ratios in radiative shocks provide higher magnetic field energy densities but also higher CR energy densities. Due to this, we can expect an approximately constant partition between the CR energy density and the magnetic field energy density during the radiative phases of evolution, until the end of the evolution of an SNR (Urošević et al. 2018). Bearing in mind these facts related to the radiative shocks, the analysis presented here can be extended to the entire SNR evolution.

Finally, it is reasonable to conclude that we can make a preliminary estimate of the evolutionary status of a newly observed SNR in a very simple and fast way by using the concept presented in this review.

6. Application of the New Concept—Examples

There were several observed SNRs, mainly extragalactic, in this decade from the Large and Small Magellanic Clouds (LMC and SMC), for which the new concept of determining the evolutionary status is applied. Here is a brief review of the published analyses.

One of the first SNRs for which this concept was used is LMC SNR J0530–7007. In the study of de Horta et al. (2012), this SNR was mainly observed by the Australia Telescope

Compact Array (ATCA). Among other observationally obtained facts, they determined the values of the surface brightness and diameter for LMC SNR J0530–7007: $\Sigma_{1\mathrm{GHz}} = 1.1 \times 10^{-21}$ W/(m^2 Hz sr) and $D = 48$ pc. By using the BV04 Σ–D diagram (see Figure 7 in de Horta et al. 2012), the authors suggested that SNR J0530–7007 is in the early Sedov phase of evolution. It is expanding into a very low-density medium. The SN explosion energy is canonical, $\sim 10^{51}$ erg. The eqp magnetic field strength is ~ 50 μG (Arbutina et al. 2012). It corresponds to a relatively young to middle-aged SNR (probably in the early Sedov phase of evolution), where the interstellar magnetic field is compressed and amplified by the strong shock that expands in a very low-density environment (i.e., the strength of the environmental magnetic field should be lower than average). The spectral index is very steep, $\alpha = 0.85$, but the spectrum appears to be peaked/curved. It is in agreement with the explanation that steeper spectra correspond to young SNRs. On the other hand, this spectrum consists of only five data points, with two at the highest frequencies with probably underestimated values. It is well established that interferometers such as ATCA will suffer from missing flux at high radio frequencies due to the missing short spacings.

The next one is LMC SNR J0529–6653. The corresponding paper (Bozzetto et al. 2012a) was published at approximately the same time as the previous paper (de Horta et al. 2012). The same procedure was done. The result is similar—this SNR is in a similar evolutionary stage and looks like J0530–7007. The values determined for $\Sigma_{1\mathrm{GHz}}$ and D, again mainly from new ATCA observations, are 2.3×10^{-21} W/(m^2 Hz sr) and 32 pc. Again, the BV04 diagram was used, and inspection of the SNR location on the Σ–D tracks leads to a possible conclusion that this SNR is in the early Sedov phase and evolves in a very low-density environment, but the SN explosion energy is higher than typical: ~ 2–3×10^{51} erg (see Figure 7. in Bozzetto et al. 2012a). The steep spectral index of 0.68 corresponds to an evolutionary young SNR. The eqp magnetic field calculated by using the Arbutina et al. (2012) calculator is again ~ 50 μG. A relatively high magnetic field strength, because of the evolution in a very low-density medium (in that case MFA effects are necessary to reach 50 μG), leads to a reliable conclusion that J0529–6653 is a relatively young to middle-aged SNR, probably in the early Sedov phase.

Also, LMC SNR J0519–6902 was observed by ATCA (Bozzetto et al. 2012b). They determined $\Sigma_{1\mathrm{GHz}} = 5.5 \times 10^{-20}$ W/(m^2 Hz sr), and $D = 8.2$ pc. From the location of this SNR on the BV04 plot, one more young SNR in the early Sedov phase was recognized. This object evolves in an environment of average density, and the initial energy of the explosion is low (see Figure 7 in Bozzetto et al. 2012b). The eqp magnetic field value is ~ 170 μG. This is the expected strength for the amplified magnetic field in a young SNR (embedded in ISM of average density). The spectral index of SNR J0519–6902 is typical for most SNRs, $\alpha = 0.53$. On the other hand, the fitted line that represents the spectrum is flatter because of the probably underestimated flux density at a lower frequency in the spectrum (408 MHz). Due to this with more reliable measurements at lower frequencies the spectral index should be steeper, closer to 0.6 which is typical for young SNRs. We have a reason to conclude that SNR J0519–6902 is a young SNR, in the early Sedov phase of evolution, which expands in the environment of average density.

De Horta et al. (2013) analyzed ATCA observations of Galactic SNR G308.3-1.4. This is the first Galactic SNR for which the concept given in this review was used. They calculated $\Sigma_{1\mathrm{GHz}} = 1.1 \times 10^{-21}$ W/(m^2 Hz sr), and $D = 34$ pc, by using distance (19 kpc) determined from Pavlović et al. (2013) Σ–D relation. SNR G308.3-1.4 is very distant object, located on the far side of the Galaxy. Location of G308.3-1.4 on the BV04 diagram suggests that it is in the early Sedov phase of evolution, expanding into an extremely low-density environment with an SN explosion energy lower than the canonical SN energy of 10^{51} erg. The spectral index of 0.68 would be expected for a young SNR. The eqp magnetic field is ~ 30 μG—the MFA effects have to be active to reach this strength because of extremely rarefied IS environment in which the SNR expands and due to this very low environmental magnetic field strength. For the same reasons, we can again conclude that this is a relatively young to middle-aged SNR, probably in the early Sedov phase of evolution.

Bozzetto et al. (2013) presented a detailed study of ATCA observations of a newly discovered LMC SNR J0533-7202. From the SNR position at the BV04 diagram ((Σ, D) = (1.1×10^{-21} W/(m^2 Hz sr), 32.5 pc)), they suggested that SNR J0533-7202 is likely to be an SNR in the late Sedov phase, with an explosion energy between 0.25 and 1×10^{51} erg, which evolves in an environment of density ~ 1 cm^{-3}. The spectral index of ~ 0.5, and the eqp magnetic field of 45 μG (the SNR expands into denser environment—this strength of the magnetic field can be reached exclusively by the compression on the strong shock front, the MFA does not need to be included), support an evolutionary older SNR in the late Sedov phase.

The next SNR in our analysis is LMC SNR J0508-6902. Among other observations at different wavelengths (optical and X), it was observed in radio again by ATCA (for details see Bozzetto et al. 2014a). This large SNR is in evolutionary terms similar to previous SNR J0533-7202. The large diameter is reached by evolution in the average density of environment ~ 0.3 cm^{-3} (BV04). Again from the BV04 diagram ((Σ, D) = (1.4×10^{-21} W/(m^2 Hz sr), 65.5 pc)), Bozzetto et al. (2014a) estimated that SNR J0508-6902 is likely to be an older SNR probably in transition between the Sedov and radiative phases of evolution. The spectral index of 0.6 (the steeper spectra should appear for older SNRs), and the magnetic field of ~ 30 μG, again support the results obtained from the evolutionary analysis based on the Σ–D tracks.

Bozzetto et al. (2014b) analyzed archival and own new ATCA observations for LMC SNR J0509-6731. For observed (Σ, D) = (1.1×10^{-19} W/(m^2 Hz sr), 7.35 pc) from BV04 plot it was estimated that this remnant is in the transition phase between the late free expansion and the early Sedov phase, with an explosion energy of 0.25×10^{51} erg, and evolving in environment of average density of 0.3 cm^{-3}. This LMC SNR has similar surface brightness and diameter to Galactic Tycho and Kepler SNRs ($\Sigma_{1\mathrm{GHz}} = 1.32 \times 10^{-19}$ W/(m^2 Hz sr), $D = 9.3$ pc; $\Sigma_{1\mathrm{GHz}} = 3.18 \times 10^{-19}$ W/(m^2 Hz sr), $D = 5.2$ pc, respectively). The steep spectral index of 0.73, and the eqp magnetic field of $\sim$170 μG support the conclusion that this is a young SNR in transition between the late free expansion and the early Sedov phase of evolution.

The first SNR from SMC for which the evolutionary status was estimated by this concept is HFPK 334 (Crawford et al. 2014). ATCA observations gave (Σ, D) = (3.6×10^{-21} W/(m^2 Hz sr), 20 pc). From BV04 $\Sigma - D$ diagram, Crawford et al. (2014) concluded that it is a young SNR expanding in a very low-density environment, with the SN explosion energy of $\sim 2 \times 10^{51}$ erg. With the spectral index of 0.6, and the eqp magnetic field of 90 μG, all three methods support that this young SNR is in transition between the late free expansion and the early Sedov phase of evolution.

For positioning of the previously reviewed eight SNRs on the $\Sigma - D$ tracks, the BV04 evolutionary paths were used. For the next couple of SNRs, the same concept is applied but using the new (P18) $\Sigma - D$ tracks presented in Figure 1, and upgraded eqp calculation from Urošević et al. (2018).

From the radio continuum survey of the SMC by using the Australian Square Kilometre Array Pathfinder (ASCAP), two candidates for SNRs were detected for the first time (Joseph et al. 2019). The observed frequencies for the entire survey are at 960 MHz (4489 detected sources) and 1320 MHz (5954 detected sources). These two newly detected SMC SNRs are: J0057-7211 and J0106-7242. Joseph et al. (2019) applied the concept from this review to determine the evolutionary status for both newly discovered SNRs. The position of these two SNR candidates on the P18 diagram ($\Sigma = 6.38 \times 10^{-22}$ and 5.38×10^{-22} W/(m^2 Hz sr), $D = 47$ and 45 pc, respectively) suggests that these SNRs are in the late Sedov phase of evolution, with an explosion energy of 1–2 $\times 10^{51}$ erg, which evolves in a rare environment of 0.02–0.2 cm^{-3}. The spectral indices are 0.75 and 0.55, respectively. Only two observed frequencies exist and therefore these two values for spectral indices are not representative enough to justify valid conclusions. From the new eqp calculation, the magnetic field strengths are 15 and 8 μG. Finally, we can conclude that these SNRs are evolutionary older SNRs in the late Sedov phase.

Additionally, the evolutionary status of LMC SNR N103B was determined by Alsaberi et al. (2019). This SNR is probably a young type Ia SNR, similar to Galactic Tycho and Kepler SNRs, and also to LMC SNR J0509-6731 (reviewed previously in this Section). For (Σ, D) = (6×10^{-19} W/(m^2 Hz sr), 6.8 pc) P18 diagram suggests transition between the late free expansion and the early Sedov phase of evolution, with an explosion energy of 1–1.5 $\times 10^{51}$ erg, which evolves in an environment with a density of 0.02–0.2 cm^{-3}. The spectral index of N103B is 0.75, the eqp magnetic field is 235 μG. Here, it should be emphasized again that for the youngest SNRs, the equipartition assumption is not that appropriate for the determination of magnetic field strength (see Urošević et al. 2018). On the other hand, the order of magnitude precision, which can be provided even for the youngest SNRs, is sufficient for the purposes of this concept. Again, all three methods suggest a young SNR in transition between the late free expansion and the early Sedov phases of evolution.

7. Reanalysis: Application of the Updated Σ–D and eqp Methods

In Section 6, BV04 Σ–D tracks are used for the study of the first eight SNRs. From the P18 study we can use the updated evolutionary paths. The main difference between BV04 and P18 tracks is in an interesting fact obtained in P18: for SNRs with the same SN explosion energy which evolve in different ambient densities appear intersections of Σ–D tracks for diameters between 10 pc and a few tens of parsecs, and due to this we can expect changes in the final determination of the evolutionary status for some SNRs. In BV04 diagram the crossings between tracks do not exist—their Σ–D tracks for different densities (again for the same SN explosion energy) ends in one point—they converge with each other. Additionally, after Urošević et al. (2018) study, the so-called "electron eqp," between the energy densities of CR electrons and magnetic fields should be used for the calculation of magnetic field strengths. Here we check eight previously analyzed SNRs (Section 6) in order to see whether there are any changes after using both updates.

For LMC SNR J0530–7007, the P18 diagram (Figure 1) suggests the following: expansion in a very low-density environment with canonical SN explosion energy. Instead of 50 μG, the electron eqp calculation gives 35 μG. In the very low-density environment, MFA is necessary process for reaching 35 μG. The final conclusion is the same as presented in Section 6. This is a relatively young to middle-aged SNR.

The position of LMC SNR J0529-6653in Figure 1 suggests again a very low-density environment. On the other hand, the SN explosion energy should be lower than standard one (contrary to the suggestion given in Section 6). Also at P18 Σ–D diagram, this SNR is located close to the evolutionary path of an older SNR in the Sedov phase expanding in an ISM of average density 0.5 cm^{-3}, and with a higher than the average SN explosion energy 2×10^{51} erg. The electron eqp magnetic field is 25 μG (instead of the previously given 50 μG). For the expansion of this SNR in an average ISM density, the magnetic

field of 25 μG can be produced only by compression of the ISM magnetic field. Here, we need a third method to make a final decision—spectral slope. The spectral index is 0.68. The slope for the ordinary older SNRs in the Sedov phase of evolution should be <0.6. Hence, the final conclusion should be the same as given in Section 6, but this result should be taken with caution.

Now we are moving onto LMC SNR J0519–6902. Different than suggested in Section 6, from Figure 1 we can conclude that this SNR evolves in lower than average density $(0.005 - 0.02)$ cm^{-3} with lower than average SN explosion energy, but in the early Sedov phase of evolution—same as concluded in Section 6. The electron eqp magnetic field is 63 μG (instead of 170 μG). Although this value is approximately 2.7 times lower than the previously obtained, for the low-density medium MFA have to be active to reach 63 μG. The final conclusion is again the same—it is a young SNR, in the early Sedov phase of evolution. The age ∼700 yr obtained in analysis of Seitenzahl et al. (2019) supports conclusion that LMC SNR J0519–6902 is young one.

The position of Galactic SNR G308.3-1.4 in Figure 1 unequivocally indicates expansion in the low-density environment (0.005–0.02) cm^{-3} with an SN explosion energy lower than the canonical SN energy of 10^{51} erg. The electron eqp magnetic field is 15 μG (previously determined 30 μG). In extremely rarefied environment, this magnetic field strength can be provided by MFA. On the other hand, similarly to the analysis for LMC SNR J0529–6653, a possible interpretation can be evolution in a denser environment, which leads to an evolutionary older SNR in the Sedov phase. Again, the spectral index of 0.68 provides that this conclusion tentatively goes to favor young to middle-aged SNRs.

LMC SNR J0533-7202 evolves in an environment of average density (Figure 1). The SN explosion energy is slightly lower than typical. The electron eqp magnetic field is 15 μG (instead of 45 μG). This supports the same conclusion as given in Section 6—an evolutionary older SNR in the late Sedov phase.

For LMC SNR J0508-6902, the P18 diagram suggests evolution in a very low-density environment (0.005 cm^{-3}), with SN explosion energy of 2×10^{51}. The difference in comparison to the suggestion given in Section 6 (the evolution in an average ISM density) leads to the conclusion that this SNR is not so evolutionary old (transition between the late Sedov and radiative phases of evolution is suggested in Section 6). This SNR is in the Sedov phase of evolution with the electron eqp field of 13 μG (instead of 30 μG given in Section 6), and a spectral index of 0.6.

The position of LMC SNR J0509-6731 in Figure 1 indicates evolution in a low-density medium ∼0.02 cm^{-3}, with low SN explosion energy. It is again lower environmental density than suggested in Section 6. The electron eqp magnetic field strength is 95 μG (170 μG in Section 6). The final conclusion is the same—young SNR in transition between the late free expansion and the early Sedov phase of evolution. This conclusion is supported by result obtained in Seitenzahl et al. (2019) - they estimated age of ∼350 yr.

Finally, for SMC SNR HFPK 334, the P18 diagram suggests evolution in the environment of average to higher density $\gtrsim$0.5 cm^{-3}, with lower SN explosion energy. The estimated ambient density in Section 6 is approximately two order of magnitude lower, and the SN explosion energy is four times higher. The electron eqp magnetic field is 38 μG (90 μG in Section 6). The spectral index is 0.6. Due to this updated analysis, this SNR is probably not a young SNR in transition between the late free expansion and the early Sedov phase of evolution, as estimated in Section 6. The presented results are consistent with the following conclusion: SMC SNR HFPK 334 is an evolutionary older SNR in the Sedov phase (with the tendency to be in transition between the late Sedov phase and radiative phases of evolution).

8. Summary

In this review, I presented:

(i) A brief overview of three methods related to radio observations, which can be combined for the purpose of making a preliminary estimate of the evolutionary status for an observed SNR.
(ii) Explanation how to apply the new concept for the preliminary determination of the evolutionary status.
(iii) Examples from literature where this concept has already been used, and additionally revision of earlier results by using the updated Σ–D and eqp analyzes (both published in 2018).

In the end, I would like to emphasize the fact that this concept for the preliminary determination of the evolutionary status of SNRs is a result of approximately 20 yr of work of the Belgrade SNR Research Group. The results which represent the basis for this review were published in more than 60 papers in the best astronomy and astrophysics journals. The theoretical fundamentals for all three methods, which are used in combination, were presented in: more than 25 papers for the Σ–D analysis, more than 10 on continuum radio spectra of SNRs, more than five for eqp method applied to SNRs. The most important of them (around 20) are cited in this review. Finally, in more than 10 papers we used the concept for determining the evolutionary stages for some observed SNRs in radio, explicitly presented in this review .

I would like to thank the members of the Belgrade SNR Research Group as these are our shared results the results set out here belong to us all: B. Arbutina, B. Vukotić, D. Onić, M. Vučetić, M. Pavlović, V. Zeković, and P. Kostić. I also would

like to thank D. Ilić and A. Ćiprijanović our internal collaborators specializing in some other fields of astrophysics, but working with us on the emission nebulae research. The concept described in this review would never be tested on the observational data without M. Filipović our main external collaborator. Also, many thanks to D. Momić, B. Arbutina, and M. Božić for thought-provoking discussions and meticulous reviewing and editing of the typescript. Finally, I would like to acknowledge the referee, John Raymond, for valuable comments which significantly improved quality of this article. I am also grateful to the Ministry of Education, Science and Technological Development of Serbia for its financial support, agreement No. 451-03-68/2022-14/200104.

ORCID iDs

Dejan Urošević https://orcid.org/0000-0003-0665-0939

References

Alsaberi, R. Z. E., Barnes, L. A., Filipović, M. D., et al. 2019, Ap&SS, 364, 204
Arbutina, B., & Urošević, D. 2005, MNRAS, 360, 76
Arbutina, B., Urošević, D., Andjelić, M. M., et al. 2012, ApJ, 746, 79
Arbutina, B., Urošević, D., Stanković, M., & Tešić, Lj. 2004, MNRAS, 350, 346
Arbutina, B., Urošević, D., Vučetić, M. M., et al. 2013, ApJ, 777, 31
Bandiera, R., & Petruk, O. 2010, A&A, 509, A34
Beck, R., & Krause, M. 2005, AN, 326, 414
Bell, A. R., Matthews, J. H., & Blundell, K. M. 2019, MNRAS, 488, 2466
Berezhko, E. G., & Völk, H. J. 2004, A&A, 427, 525, (BV04)
Bozzetto, L. M., Filipović, M. D., Crawford, E. J., et al. 2012a, MNRAS, 420, 2588
Bozzetto, L. M., Filipovic, M. D., Urosevic, D., et al. 2012b, SerAJ, 185, 25
Bozzetto, L. M., Filipović, M. D., Crawford, E. J., et al. 2013, MNRAS, 432, 2177
Bozzetto, L. M., Kavanagh, P. J., Maggi, P., et al. 2014a, MNRAS, 439, 1110
Bozzetto, L. M., Filipović, M. D., Urošević, D., et al. 2014b, MNRAS, 440, 3220
Bozzetto, L. M., Filipović, M. D., Vukotić, B., et al. 2017, ApJS, 230, 2
Crawford, E. J., Filipović, M. D., McEntaffer, R. L., et al. 2014, AJ, 148, 99
de Horta, A. Y., Filipović, M. D., Bozzetto, L. M., et al. 2012, A&A, 540, A25
De Horta, A. Y., Collier, J. D., Filipović, M. D., et al. 2013, MNRAS, 428, 1980
Joseph, T. D., Filipović, M. D., et al. 2019, MNRAS, 490, 1202
Guseinov, O. H., Ankay, A., Sezer, A., et al. 2003, A&AT, 22, 273
Kostić, P., Vukotić, B., Urošević, D., et al. 2016, MNRAS, 461, 1421
Luken, K. J., Filipović, M. D., Maxted, N. I., et al. 2020, MNRAS, 492, 2606
Onić, D., Urošević, D., Arbutina, B., et al. 2012, ApJ, 756, 61
Onić, D. 2013, Ap&SS, 346, 3
Onić, D., & Urošević, D. 2015, ApJ, 805, 119
Pacholczyk, A. G. 1970, Radio Astrophysics (Series of Books in Astronomy and Astrophysics) (San Francisco, CA: Freeman)
Pavlović, M. Z., Urošević, D., Vukotić, B., et al. 2013, ApJS, 204, 4
Pavlović, M. Z., Dobardžić, A., Vukotić, B., et al. 2014, SerAJ, 189, 25
Pavlović, M. Z. 2017, MNRAS, 468, 1616
Pavlović, M. Z., Urošević, D., Arbutina, B., et al. 2018, ApJ, 852, 84
Raymond, J. C., Slavin, J. D., Blair, W. P., et al. 2020, ApJ, 903, 2
Seitenzahl, I. R., Ghavamian, P., Laming, J. M., et al. 2019, PhRvL, 123, 041101
Shklovskii, I. S. 1960a, AZh, 37, 256
Shklovskii, I. S. 1960b, AZh, 37, 369
Tutone, A., Ballet, J., Acero, F., et al. 2021, A&A, 656, A139
Urošević, D. 2000, Ph.D. Thesis, University of Belgrade
Urosević, D. 2002, SerAJ, 165, 27
Urošević, D. 2003, Ap&SS, 283, 75
Urošević, D., Duric, N., & Pannuti, T. 2003a, SerAJ, 166, 61
Urošević, D., Duric, N., & Pannuti, T. 2003b, SerAJ, 166, 67
Urošević, D. 2005, PASRB, 5, 113
Urošević, D., & Pannuti, T. G. 2005, APh, 23, 577
Urošević, D., Pannuti, T. G., Duric, N., et al. 2005, A&A, 435, 437
Urošević, D., Pannuti, T. G., & Leahy, D. 2007, ApJL, 655, L41
Urošević, D., Vukotić, B., Arbutina, B., et al. 2010, ApJ, 719, 950
Urošević, D. 2014, Ap&SS, 354, 541
Urošević, D., Pavlović, M. Z., & Arbutina, B. 2018, ApJ, 855, 59
Urošević, D. 2020, NatAs, 4, 910
Vink, J., & Laming, J. M. 2003, ApJ, 584, 758
Vukotić, B., Arbutina, B., & Urošević, D. 2007, RMxAA, 43, 33
Vukotić, B., Jurković, M., Urošević, D., et al. 2014, MNRAS, 440, 2026
Vukotić, B., Ćiprijanović, A., Vučetić, M. M., et al. 2019, SerAJ, 199, 23